Theoretical and experimental investigation of a quadspectral nonlinearity indicator

Kyle G. Miller[1, a)], Brent O. Reichman[1], Kent L. Gee[1], Tracianne B. Neilsen[1], and Anthony A. Atchley[2]
[1]*Department of Physics and Astronomy, Brigham Young University, Provo, UT 84602, USA*
[2]*Graduate Program in Acoustics, The Pennsylvania State University, University Park, PA 16802, USA*

[a)]kglenmiller@gmail.com

The effects of nonlinearity on the power spectrum of jet noise can be directly compared with those of atmospheric absorption and geometric spreading through an ensemble-averaged, frequency-domain version of the generalized Burgers equation (GBE) [B. O. Reichman et al., J. Acoust. Soc. Am. 136, 2102 (2014)]. The rate of change in the sound pressure level due to the nonlinearity, in decibels per jet nozzle diameter, is calculated using a dimensionless form of the quadspectrum of the pressure and the squared-pressure waveforms. In this paper, this formulation is applied in detail to atmospheric propagation of a spherically spreading, initial sinusoid and unheated model-scale supersonic (Mach 2.0) jet data. The rate of change in level due to nonlinearity is calculated and compared with estimated effects due to absorption and geometric spreading. Comparing these losses with the change predicted due to nonlinearity shows that absorption and nonlinearity are of similar magnitude in the geometric far field, where shocks are present, which causes the high-frequency spectral shape to remain unchanged. Nonlinear effects are compared for engine conditions of Mach 0.85 and Mach 1.8 as well. Both the Mach-1.8 and Mach-2.0 data exhibit nonlinear trends that slow the decay of the waveform compared to absorption and spreading alone.

I. INTRODUCTION

Characterizing nonlinearity in jet noise has traditionally involved comparison of the power spectral density (PSD) along propagation radials. This approach not only necessitates several microphones placed far apart relative to the jet diameter, but the comparison naturally incorporates other effects that influence PSD evolution. Such effects include atmospheric absorption and geometric spreading from a directional, extended source, and in an outdoor measurement also ground reflections and wind and temperature gradients. These factors make it difficult to isolate nonlinear effects on PSD evolution. Other nonlinearity analysis techniques have been previously explored,[1-3] but this paper focuses on the use of a quadspectral nonlinearity indicator to determine the presence and importance of nonlinearity with a measurement at a single location.

Morfey and Howell[4] introduced the dimensionless nonlinearity indicator known as "Q/S," based on the ensemble-averaged, frequency-domain version of the generalized Burgers equation for spherical spreading,

$$\frac{Q}{S} = \frac{Q_{pp^2}}{p_{\mathrm{rms}} S_{pp}} = \frac{\mathrm{Im}\left\{\lim_{T\to\infty} \frac{1}{T} E[\mathcal{F}^*\{p(t)\}\mathcal{F}\{p^2(t)\}]\right\}}{p_{\mathrm{rms}} S_{pp}}, \tag{1}$$

where Q_{pp^2} is the quadspectral density between the pressure and squared pressure waveforms, S_{pp} is the pressure autospectral density, p_{rms} is the root-mean-square pressure, and $\mathcal{F}$ denotes a Fourier transform. Although Morfey and Howell and others have used Q/S and related indicators to demonstrate the presence of nonlinear propagation effects, a quantitative expression involving Q/S has been recently found[5] for the change in sound pressure level spectrum, L_p, with distance, r,

$$\frac{\partial L_p}{\partial r} = -10\log_{10}(e) \cdot \left(\frac{2m}{r} + 2\alpha + \frac{\omega\beta p_{\mathrm{rms}}}{\rho_0 c_0^3}\frac{Q}{S}\right) = \nu_S + \nu_\alpha + \nu_N\,. \tag{2}$$

that may be written as

In Eq. (2), $10\log_{10}(e) \approx 4.34$; $m = 0$, 0.5, or 1 for planar, cylindrical, or spherical waves, respectively; α is the linear absorption coefficient; β is the coefficient of nonlinearity; ρ_0 is the equilibrium density of air; c_0 is the speed of sound; and ν_S, ν_α, and ν_N represent the frequency-dependent spatial rate of changes in L_p due to spreading, absorption, and nonlinearity, respectively.

Other analyses of jet noise have used Q/S to show the presence of nonlinearity,[3, 6, 7] but have not been extended to the quantitative expression in Eq. (2), which has only treated analytical plane-wave cases.[5] This paper first presents a quantitative analysis of an initial sinusoid numerically propagated with spherical spreading and atmospheric absorption using a numerical implementation of the GBE.[8] Analysis of noise from an anechoic, laboratory scale, ideally expanded, Mach-2.0

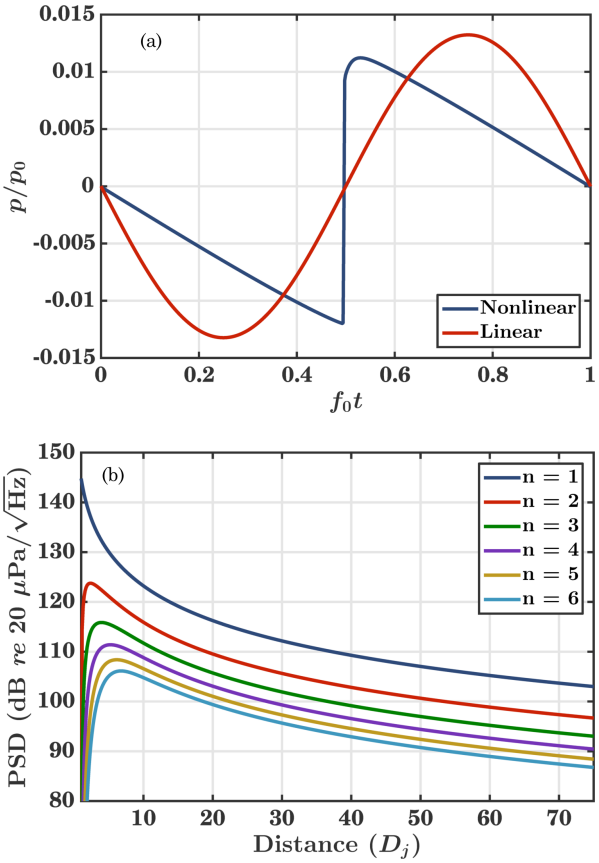

FIG 1. (a) Comparison of nonlinearly propagated wave at 75 D_j and the corresponding linear approximation. (b) Spectral amplitude of six harmonics. Each harmonic peaks at a successively larger distance from the source.

unheated jet is also presented. Both analyses show that ν_N is largest in the near-field region, then becomes comparable to absorption and spreading in the far field.

II. SINUSOID PROPAGATION ANALYSIS

To create a simulation similar to the model-scale jet experiment, a sinusoidal waveform was propagated numerically using the GBE. Unlike the jet noise case, which exhibits range and frequency-dependent geometric spreading, spherical spreading is assumed at all distances. The distance is scaled with respect to a jet nozzle diameter (D_j), equal to 3.5 cm. The atmospheric conditions were taken to be the same as in the experiment, with temperature at 22.9°C, atmospheric pressure at 96.8 kPa, and relative humidity at 53%. The fundamental frequency of the wave was 4 kHz with amplitude of 22 kPa at 1 D_j, so as to approximate the rms amplitude of the jet data at 10 D_j. For accuracy in the calculations, a sampling frequency of 88 MHz was used with 2^{16} total samples. Figure 1 (a) compares the nonlinearly propagated wave with the linear approximation (spreading and atmospheric absorption). Relative to linear propagation, significant wave steepening has occurred along with a slight decrease in the peak-to-peak pressure. Figure 1 (b) shows the evolution of the harmonics in the waveform. Note the delayed onset of higher harmonics, with each harmonic reaching its maximum amplitude at successively larger distances from the source.

The calculations of ν_s, ν_α, and ν_N in Eq. (2) were carried out using the distance, frequency, assumed atmospheric conditions, and propagated waveform. The terms, along with their sum, are shown in Fig. 2 as a function of distance for the fundamental, second harmonic, and tenth harmonic. These two harmonics have frequencies similar to those analyzed in the jet noise case. In Fig. 2, a solid black line shows the sum of ν_s, ν_α, and ν_N, and the red circles represent the

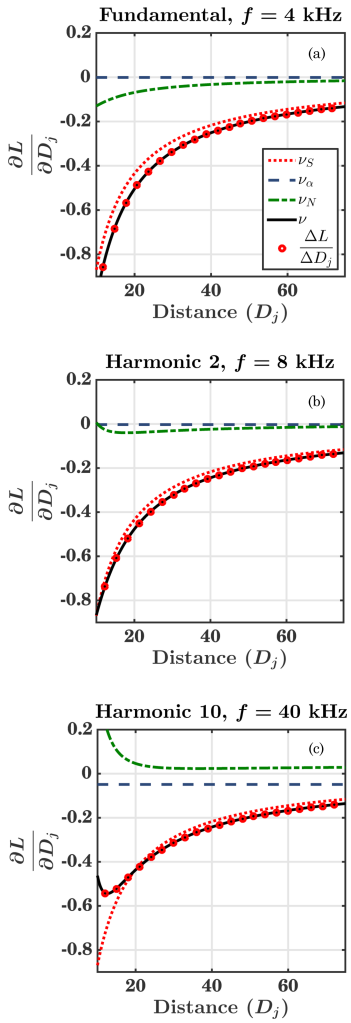

FIG 2. Comparison of ν values for the (a) fundamental, (b) second harmonic, and (c) tenth harmonic of the nonlinearly propagated waveform. Close to the source, harmonic strength is dominated by nonlinearity. Geometric spreading becomes the dominant effect at larger distances. For the tenth harmonic in (c), all three effects are of similar magnitude in the far field.

numerically calculated derivative from the curves in Fig. 1 (b). The percent error between the two is less than 1% for all values shown. Very close to the source, ν_N is positive for all harmonics as they are first generated nonlinearly. However, nonlinear losses at the shock and energy transfer to even higher frequencies causes ν_N to eventually go negative for some of the harmonics, as seen in Fig. 2 (b). For the tenth harmonic, ν_N decreases but remains positive away from the source. As pointed out by Blackstock,[9] the harmonic amplitudes in a nonlinear wave undergoing unsteepening in the "old age" region decay more slowly than a linearly propagating wave. For a plane wave experiencing atmospheric absorption and nonlinear effects (no spreading), this decay proceeds as $e^{-n\alpha x}$ instead of $e^{-n^2\alpha x}$, where α is the linear absorption coefficient and n is the harmonic number. Because the nonlinear decay for a wave of this type would be slower than that from absorption alone, ν_N would be positive in the far field.

A spherically spreading wave, however, decays as $r^{-n}e^{-n\alpha r}$ instead of $r^{-1}e^{-n^2\alpha r}$, which Blackstock points out to be a weaker decay than without nonlinearity.[9] The difference in decay rates is given by ν_N, which should therefore be positive in the far field to give a slower decay. In Fig. 2 (a), ν_N remains negative because energy is continually removed from the fundamental to nonlinearly generate the higher harmonics. Figure 2 (b) has ν_N also negative for a similar reason: energy is removed from this harmonic to generate higher frequency content. However, approaching 70 D_j the value of ν_N appears to be increasing and becoming positive, rather than asymptotically converging to zero as in 2 (a). This is confirmed in Fig. 2 (c), where ν_N converges to a positive number in the far field. This indicates a slower decay than that expected from spreading and absorption alone.

III. JET NOISE ANALYSIS

Laboratory-scale jet noise data were collected in an anechoic chamber on an ideally expanded, Mach-2.0, unheated jet of nozzle diameter 3.5 cm. Waveforms, sampled at 192 kHz, were acquired between 10-75 jet nozzle diameters (D_j) and 80° and 150° (relative to upstream axis) with a 3.18 mm and 6.35 mm microphone array whose origin was located 4 D_j downstream of the nozzle exit. This origin is upstream from the expected overall noise source region,[10] but facility configuration constraints required this positioning. Figure 3 (a) shows the measured power spectral densities (PSD) along 145°, which is the maximum far-field radiation angle. A shift in peak frequency is observed along the radial from 10 to 60 D_j, due to those microphones being in the geometric near field of a source with frequency-dependent source

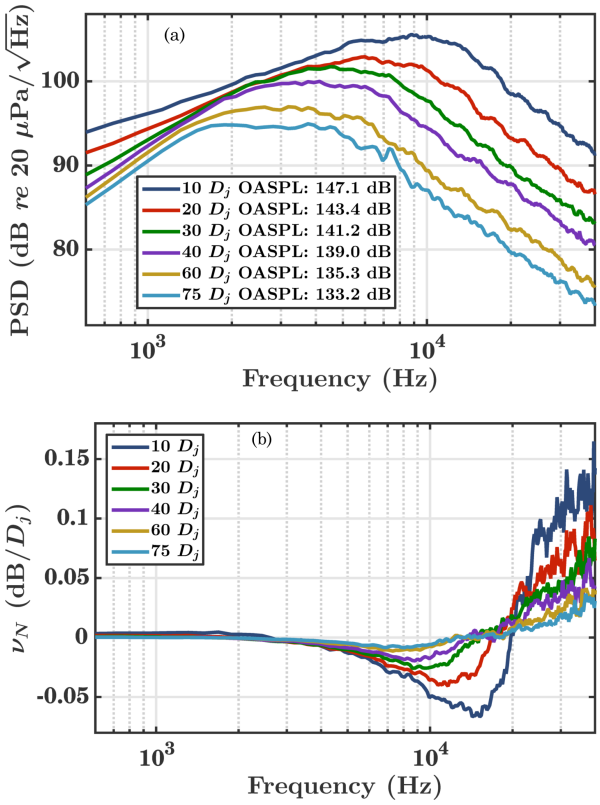

FIG 3. (a) Measured spectra along 145°, showing the downward frequency shift along the maximum far-field radiation angle. (b) Spectral plots for ν_N. A corresponding frequency shift occurs for where ν_N changes sign.

location, directivity, and spreading rate. It is important to note that this downward shift in peak frequency is not related to nonlinear effects (see discussion regarding Fig. 4 of Ref. 11). For example, low-frequency noise is generated farther downstream from the nozzle than is high-frequency noise,[10] so their propagation radials are different from each other and from the microphone array before converging at ~60 D_j. Between 10-20 kHz the roll-off changes from ~28 dB/octave at 10 D_j, the decay rate for large-scale structure radiation,[11] to ~20 dB/octave, typical of shock-containing noise.[12] This spectral shape of the high frequencies remains fairly constant with distance, indicating that the energy losses due to absorption and energy gains due to nonlinearity are of similar magnitude; this is shown quantitatively below.

Figure 3 (b) shows ν_N along the same radial. Negative and positive values of ν_N indicate loss of energy and gain in energy due to nonlinearity, respectively. The frequency at which the sign of ν_N changes from negative to positive tracks the downward trend in PSD peak frequency with propagation into the far field. This indicates that the spectral peak at a given location drives nonlinear energy transfer to higher

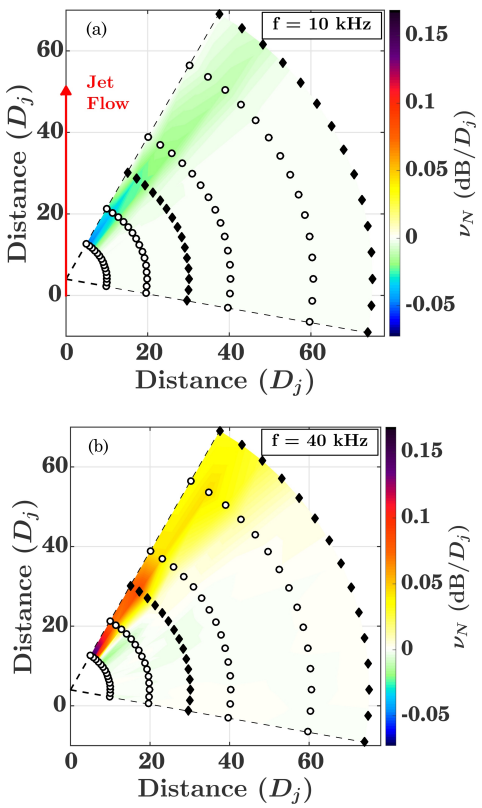

FIG 4. Spatial maps of ν_N for (a) 10 kHz and (b) 40 kHz. Circles represent 3.18 mm mics and filled diamonds 6.35 mm mics.

frequencies, similar to the sinusoid example shown previously. Note that with increased distance from the source, the frequency at which ν_N changes from negative to positive decreases. This is reminiscent of the trend in Fig. 2 (b): approaching the far field in the simple sinusoidal case, ν_N tends to a positive value for all harmonics but the fundamental. Broadband noise is more complicated, but a similar trend is visible in Fig. 3 (b): with increased distance from the source, more frequencies have positive values for ν_N . The consistently negative values correspond to the spectral peaks of the noise causing the nonlinear harmonic generation. Perhaps with measurements at increased distances from the nozzle, ν_N would transition to positive values at even lower frequencies.

The spatial maps of ν_N in Figs. 4 (a-b), created using a linear interpolation of the color scheme, quantitatively confirm that nonlinear effects are localized at angles near the maximum radiation direction, as indicated by prior analyses.[6, 13, 14] Along the principal radiation lobe, the energy loss rate (~ -0.01 to -0.05 dB/D_j) at 10 kHz and gain rate at 40 kHz (~ +0.03 to +0.1 dB/D_j) are very similar in magnitude to the sinusoid example. Similar to the numerically

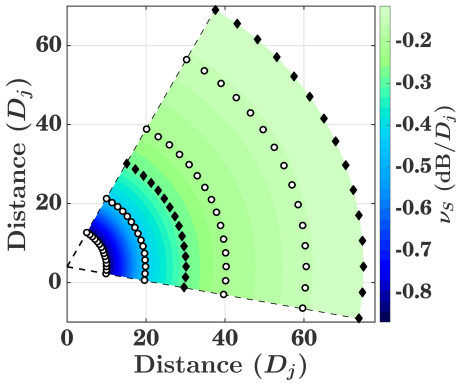

FIG 5. Spatial map of ν_S (constant with frequency), which dominates both nonlinearity and absorption.

propagated sine wave, nonlinearity is more dominant than absorption close to the source, but the two effects are close to the same strength in the far field. Absorption gives a change of only -0.004 dB/D_j at 10 kHz and -0.05 dB/D_j at 40 kHz. Once again, the value of ν_N stays positive at 40 kHz because the observed decay of a spherically spreading nonlinear wave is less than that predicted by spreading and absorption alone.

Figure 4 (b) shows a small negative region around the propagation radial at 130°, where energy is still being lost at 40 kHz. The peak frequency in this region is about twice that of the principle radiation radial, and energy is being lost at this frequency to higher harmonic generation. Figure 5 shows that ν_S, the change due to spherical spreading ($m = 1$ in Eq. [(2]), is almost an order of magnitude stronger than both nonlinearity and absorption at all microphones in the tested region.

Data were also collected at Mach 0.85 and Mach 1.8, and the overall sound pressure levels (OASPL) are compared in Fig. 6. A significant increase in level is observed between the Mach-0.85 and Mach-1.8 data. The levels are similar for the Mach-1.8 and Mach-2.0 data, but a slight change in directivity is observed. The principal radiation lobe at Mach 2.0 is stronger, thicker, and projected further away from the jet plume. However, Fig. 6 (b) for the Mach-1.8 data shows a secondary radiation lobe projecting at about 125°, different from the Mach-2.0 data.

The change in OASPL also reflects a change in the nonlinear behavior for these three jet conditions as well. Spatial maps of ν_N are shown in Fig. 7 for the three conditions. Figure 7 (a) shows almost no nonlinearity present in the waveforms, and the spatial plot contains only noise. The maps for Figs. 4 (b) and 7 (b) are plotted on the same color scale for direct comparison. Both plots contain a region of intense nonlinear growth within about 30 D_j of the nozzle and along the principal radiation lobe, corresponding to shock formation. In addition, the value for ν_N remains positive in the far field and along the radiation lobes for both engine conditions. This indicates a slower decay than predicted

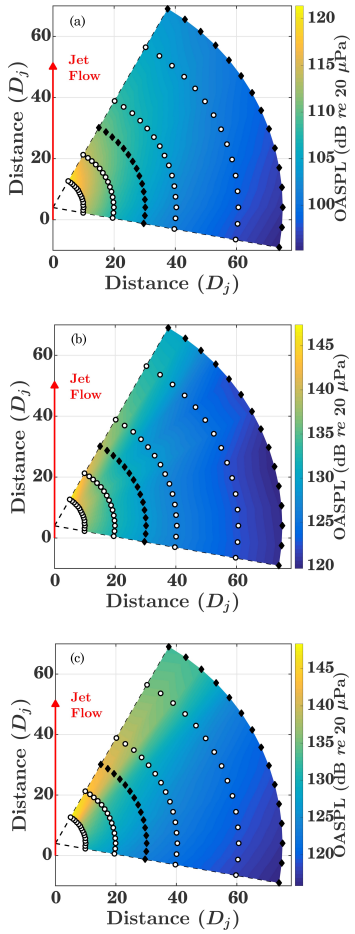

FIG 6. Overall sound pressure levels (OASPL) for (a) Mach-0.85, (b) Mach-1.8, and (c) Mach-2.0 data. A substantial increase in level is observed from (a) to (b), and a slight change in directivity is observed from (b) to (c).

by absorption and spreading alone, typical of an unsteepening wave in the "old age".[9] A positive ν_N value is even observed along the secondary radiation lobe in the Mach-1.8 data. However, the strength of the nonlinearity is overall greater at Mach 2.0.

IV. CONCLUSION

The Morfey-Howell[4] nonlinearity indicator, Q/S, has been extended to a quantitative comparison of nonlinear effects with those of spreading and absorption for a spherically spreading, initially sinusoidal case and for supersonic model-scale jet noise. The analysis shows that nonlinearity is strongest close to the source, but approaches similar magnitude as absorption in the far field. Prior studies of the jet data have revealed that acoustic shocks form with propagation into the far field,[14] and that the high-frequency spectral energy is increasingly due to the shocks.[13] This study confirms that the unchanging high-frequency spectral roll-off is

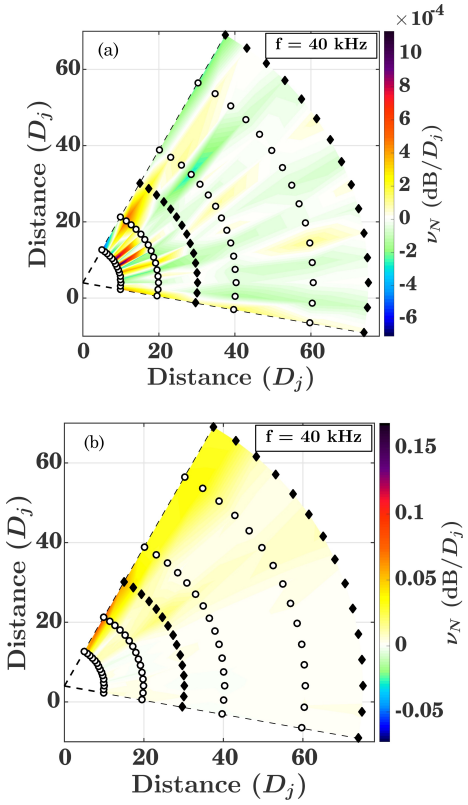

FIG 7. Spatial maps of ν_N for 40 kHz at (a) Mach 0.85 and (b) Mach 1.8. Part (a) exhibits no nonlinearity, with the plot containing only noise. Part (b) and Fig. 4 (b) are plotted on the same color scale for comparison.

due to comparable magnitudes of the loss due to absorption and the gain due to nonlinear generation as the shocks propagate. In fact, a positive value for the nonlinearity indicator ν_N shows that the overall decay of the waveform is less than predicted by absorption and spreading alone.

ACKNOWLEDGMENTS

This work was supported by the U.S. Office of Naval Research.

[1]W. J. Baars, C. E. Tinney, M. S. Wochner and M. F. Hamilton, "On cumulative nonlinear acoustic waveform distortions from high-speed jets," J. Fluid Mech. **749**, 331-366 (2014).
[2]S. A. McInerny, M. Downing, C. Hobbs, M. James and M. Hannon, "Metrics that characterize nonlinearity in jet noise," AIP Conf. Proc. **838**, 560-563 (2006).
[3]S. A. McInerny and S. M. Ölçmen, "High-intensity rocket noise: Nonlinear propagation, atmospheric absorption, and characterization," J. Acoust. Soc. Am. **117**, 578-591 (2005).
[4]C. L. Morfey and G. P. Howell, "Nonlinear propagation of aircraft noise in the atmosphere," AIAA Journal **19**, 986-992 (1981).

[5]B. O. Reichman, K. L. Gee, T. B. Neilsen and K. G. Miller, "Quantitative analysis of a frequency-domain nonlinearity indicator," J. Acoust. Soc. Am. (submitted 2015).
[6]K. L. Gee, A. A. Atchley, L. E. Falco and M. R. Shepherd, "Nonlinearity analysis of model-scale jet noise," AIP Conf. Proc. **1474**, 307-310 (2012).
[7]B. P. Petitjean, K. Viswanathan and D. K. McLaughlin, "Acoustic pressure waveforms measured in high speed jet noise experiencing nonlinear propagation," Int. J. Aeroacoust. **5**, 193-215 (2006).
[8]K. L. Gee, "Prediction of nonlinear jet noise propagation," Ph. D. Thesis, Pennsylvania State University, 2005.
[9]D. T. Blackstock, "Once Nonlinear, Always Nonlinear," AIP Conf. Proc. **838**, 601-606 (2006).
[10]C. K. W. Tam, K. Viswanathan, K. K. Ahuja and J. Panda, "The sources of jet noise: experimental evidence," J. Fluid Mech. **615**, 253-292 (2008).
[11]T. B. Neilsen, K. L. Gee, A. T. Wall and M. M. James, "Similarity spectra analysis of high-performance jet aircraft noise," J. Acoust. Soc. Am. **133**, 2116-2125 (2013).
[12]S. N. Gurbatov and O. V. Rudenko, "Statistical phenomena," in *Nonlinear Acoustics*, (American Press, San Diego, 1998), pp. 377-398.
[13]K. L. Gee, A. A. Atchley, L. E. Falco, M. R. Shepherd, L. S. Ukeiley, B. J. Jansen and J. M. Seiner, "Bicoherence analysis of model-scale jet noise," J. Acoust. Soc. Am. **128**, EL211-EL216 (2010).
[14]K. L. Gee, T. B. Neilsen and A. A. Atchley, "Skewness and shock formation in laboratory-scale supersonic jet data," J. Acoust. Soc. Am. **133**, EL491-EL497 (2013).